

TECHNICAL NOTES

Wall-to-fluid coefficients for fixed bed heat and mass transfer

ANTHONY G. DIXON and LEONARD A. LABUA

Department of Chemical Engineering, Worcester Polytechnic Institute, 100 Institute Road,
Worcester, MA 01609, U.S.A.

(Received 1 May 1984 and in revised form 25 July 1984)

NOMENCLATURE

- A proportionality factor, defined in equation (5)
- b exponent on Re , defined in equation (5)
- Bi_m mass transfer wall Biot number
- d_p sphere diameter
- d_{pv} diameter of equivalent volume sphere (hollow cylinders are treated as though full, the hole is counted as solid)
- d_i bed diameter
- Nu_{wf} wall-to-fluid Nusselt number
- Pe_{rf} fluid-phase heat transfer Peclet number
- Pe_{rm} mass transfer Peclet number
- Pr Prandtl number
- R bed radius
- Re Reynolds number, based on d_{pv}
- Sc Schmidt number
- Sh_{wf} Sherwood number, based on d_{pv}

All transport coefficients are based on unit void plus non-void area perpendicular to the transfer direction.

INTRODUCTION

THE MODELLING of heat transfer in fixed beds is an important step in the design effort, especially for the beds of low tube-to-particle diameter ratio (d_i/d_p) used in shell-and-tube reactors. A pseudohomogeneous two-dimensional model has been widely used for this purpose [1], which accounts for transfer of energy by bulk flow in the axial direction and dispersion and conduction in the radial direction.

The parameters of this model are termed effective, in that many transport mechanisms are lumped together and represented by a single radial conductivity and a single wall transfer coefficient. Empirical correlation of these quantities has been difficult, due to the many competing phenomena they embrace. A model hierarchy approach has been advocated [1], in which the effective parameters are related to individual-phase transport coefficients. This approach requires reliable correlations for fluid-phase and solid-phase heat transfer parameters.

The contribution of the fluid phase to heat transfer has usually been obtained by invoking heat-mass analogies

$$Pe_{rm} = Pe_{rf} \tag{1}$$

$$\frac{Sh_{wf}}{Re Sc^{1/3}} \equiv j_D = j_H \equiv \frac{Nu_{wf}}{Re Pr^{1/3}} \tag{2}$$

and carrying out mass transfer experiments to determine Pe_{rm} and Sh_{wf} . A previous study [2] for low d_i/d_p beds of spheres gave the results for Sh_{wf} reproduced here in Fig. 1, which were correlated by

$$Sh_{wf} = [1.0 - 1.5(d_p/d_i)^{1.5}] Sc^{1/3} Re^{0.59} \tag{3}$$

The object of the present work is to obtain corresponding results for low d_i/d_p beds of full cylinders (pellets) and hollow cylinders (rings), which are more realistic shapes for catalyst supports.

EXPERIMENTAL

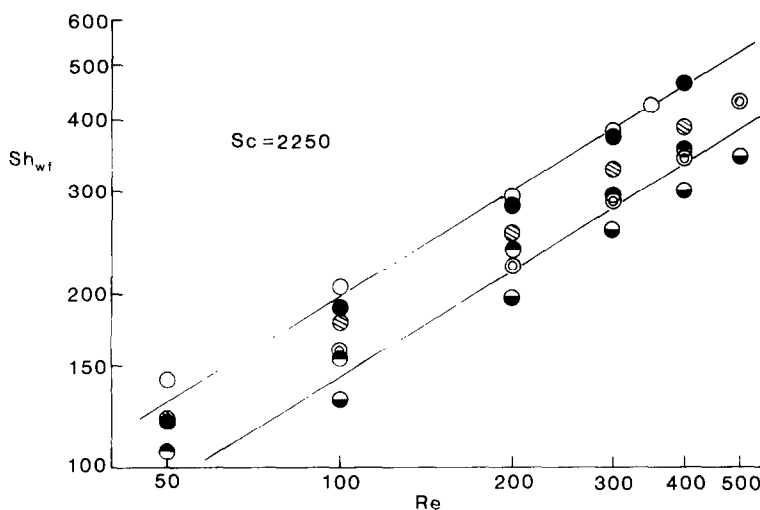
The equipment and procedure used in this work have been extensively described and discussed previously [2]. In brief, a copper tube 76 mm I.D. and 203 mm long was coated with benzoic acid on the inside wall, placed in the test rig and packed. Above this packed coated section was a 152-mm-long packed, uncoated calming section. Details of the various packings used are given in Table 1. The packing rested on a brass wire support grid at the bottom of the coated section. Immediately below this was a 152-mm-long annular splitter, which contained concentric tubes of 25.4 mm and 50.8 mm I.D., thus allowing three annular radially-averaged measurements.

The column was filled with water and air removed by a bleeding procedure. Water flow downwards through the column was started, and the flow rates through the annuli controlled by valves and metered by rotameters on the exit lines from the annuli. A uniform velocity profile was assumed when calculating annular flow rates, although non-uniformity is likely for low d_i/d_p . No reliable measurements of fixed bed velocity profiles were available, and the limitations of the plug-flow assumption are discussed later. A thorough study of this point was made in previous work [2].

The column was operated and exit samples of water monitored for benzoic acid concentration until steady state was reached, when final samples were taken. The concentrations of the samples were obtained by measuring absorbances with a UV-spectrophotometer at a wavelength of 271 nm. For each packing size four to five flow rates were used, in the range $50 < Re < 500$. All runs were repeated with a new coating, and the data analyzed simultaneously, so that the results represent averages over re-packed beds.

Table 1. Packing materials represented in Figs. 1-4

Symbol	Packing	d_i/d_{pv}
○	6.4 mm nylon spheres	11.8
⊗	8.0 mm nylon spheres	9.4
●	9.6 mm nylon spheres	7.8
●	12.7 mm nylon spheres	5.8
⊙	19.0 mm polystyrene spheres	3.9
●	25.4 mm nylon spheres	2.9
▤	8 mm × 8 mm × 6 mm glass rings	8.2
▤	6 mm × 6 mm × 4 mm glass rings	10.9
▤	12.7 mm × 12.7 mm × 6.4 mm ceramic rings	5.0
▤	9.6 mm × 9.6 mm × 4.8 mm ceramic rings	6.8
▤	12.7 mm × 12.7 mm × 6.4 mm aluminum rings	5.0
▤	9.6 mm × 9.6 mm × 4.8 mm aluminum rings	6.8
■	12.7 mm × 12.7 mm aluminum pellets	5.0
▤	9.6 mm × 9.6 mm aluminum pellets	6.8
□	6.4 mm × 6.4 mm aluminum pellets	10.2

FIG. 1. Sh_{wf} for spherical packings [2].

The solution to the material balance equations was averaged over a radial annulus [2] and the two parameters Pe_{rm} and Bi_m estimated by least-squares fitting of the model to the data. The Sherwood number was then obtained from

$$(Bi_m) \left(\frac{d_p}{R} \right) = (Sh_{wf}) \left(\frac{Pe_{rm}}{Re Sc} \right) \quad (4)$$

The model used had previously been shown to be statistically adequate to describe the mass transfer experiments [2].

DISCUSSION OF RESULTS

Dixon *et al.* [2] showed that the radial mass Peclet number (Pe_{rm}) estimates were very sensitive to the velocity profile assumed in setting the exit flow rates from the annuli. This parameter, therefore, cannot be reliably obtained from the present experiments. The Sherwood number, computed from equation (4), was relatively insensitive to velocity profile, however, and the values of this parameter found here are presented in Figs. 2 and 3.

The Sh_{wf} for each packing were correlated against Re in the form

$$Sh_{wf} = A(Sc)^{1/3}(Re)^b \quad (5)$$

and values of the exponent b and proportionality constant A obtained. The data from Figs. 1–3 gave the following ranges of exponents

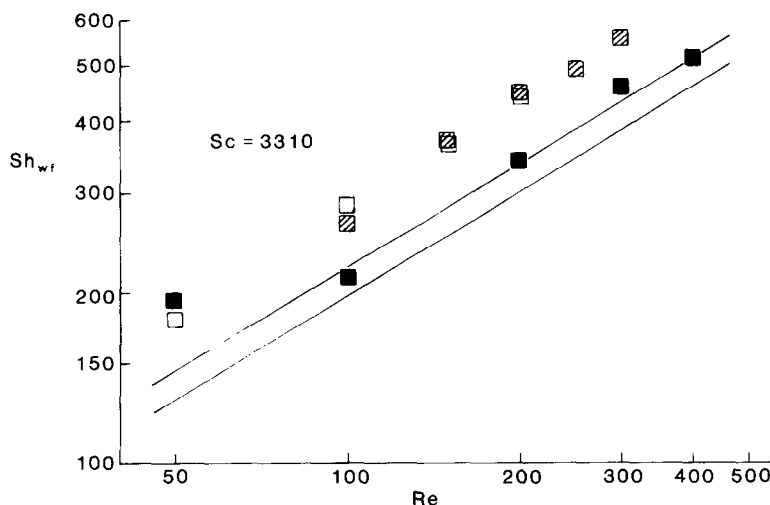
$$0.55 < b < 0.64 \quad (\text{spheres})$$

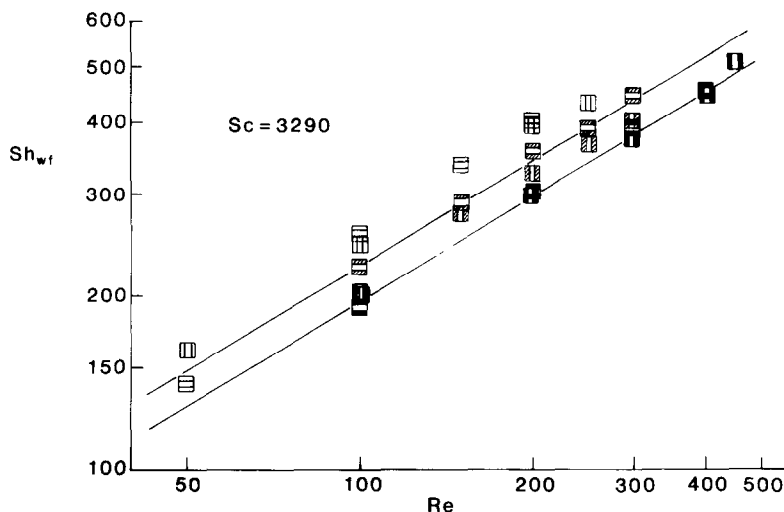
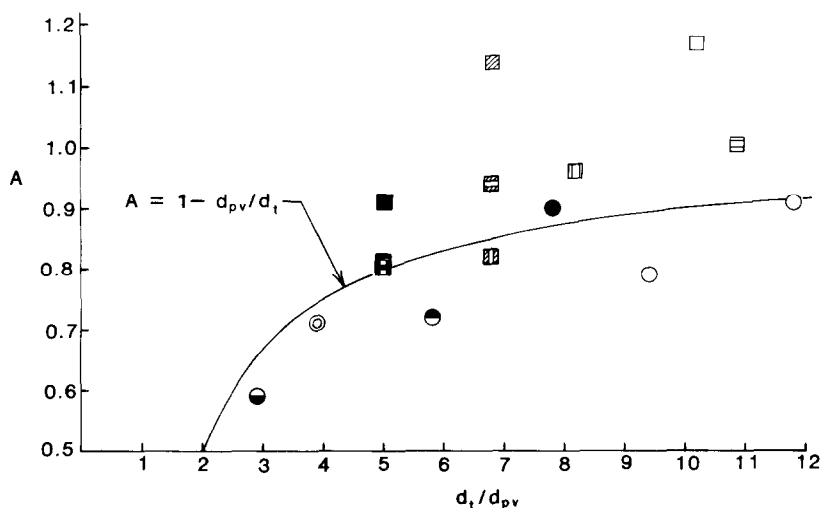
$$0.62 < b < 0.68 \quad (\text{full cylinders})$$

$$0.59 < b < 0.66 \quad (\text{hollow cylinders})$$

In view of the scatter in the data and the confidence intervals on the Sh_{wf} , it was decided that the data here did not justify the development of individual correlations for spheres, pellets and rings. Accordingly, an average exponent of $b = 0.61$ was chosen and the data re-fitted by equation (5) with this fixed value. The proportionality constants A so obtained are shown in Fig. 4.

Although there is some ordering of the values of A (in general: cylinders > hollow cylinders > spheres, in magnitude), it was again felt that a simple form would be adequate to give the dependence of A upon d_i/d_{pv} . If the correlations reviewed in [3] are manipulated into the form of equation (5) with $b = 0.61$, as shown previously in [2], then the higher d_i/d_p studies of beds of spheres suggest that $A \rightarrow 1$ as $d_i/d_{pv} \rightarrow \infty$, and this together with empirical fitting of the main body of

FIG. 2. Sh_{wf} for full cylinder packings.

FIG. 3. Sh_{wf} for hollow cylinder packings.FIG. 4. Proportionality constant dependence on d_t/d_{pv} .

values for A led to the final form

$$Sh_{wf} = (1 - d_{pv}/d_t)(Sc)^{1/3}(Re)^{0.61}(Re > 50) \quad (6)$$

which is also shown in Fig. 4.

A comparison may be made between the predictions of equation (6) and the experimental data of Figs. 1–3. The lines shown correspond to the highest and lowest d_t/d_{pv} packings for each shape. For individual data points, the average relative error is 10% of the true value. For full cylinders the prediction is up to 25% low, however for spheres and hollow cylinders predictions closer than the 10% are consistently achieved. It is noteworthy that the exponent of 0.61 found here is in excellent agreement with the high d_t/d_p results of electrochemical limiting current experiments in beds of spheres [3], which show exponents in the range 0.6–0.63. There is also excellent agreement with the low d_t/d_p work of Rao and Rao [4], who studied rings, saddles and spheres in square beds for the range $5.7 < d_t/d_p < 13$, and who obtained an exponent of 0.60. They did not attempt to include a d_t/d_p -dependence in their results, although there was some spread of data points around their correlating line. The relative independence of Sh_{wf} of the packing shapes is also interesting; a related result in studies of solid conduction in fixed beds [5] gave the wall-to-solid Biot number also as a single correlation in terms of d_t/d_{pv} for beds of spheres, pellets and rings with low conductivity packings.

CONCLUSIONS

A simple formula for Sh_{wf} has been found, in terms of d_t/d_{pv} and Re , which gives reasonable accuracy for three different packing types. A corresponding formula for Nu_{wf} follows immediately by the heat-mass analogy. Improved predictions of effective heat transfer parameters may be anticipated through use of the formulas presented here.

REFERENCES

1. A. G. Dixon and D. L. Cresswell, Theoretical prediction of effective heat transfer parameters in packed beds, *A.I.Ch.E. JI* **25**, 663–676 (1979).
2. A. G. Dixon, M. A. DiCostanzo and B. A. Soucy, Fluid-phase radial transport in packed beds of low tube-to-particle diameter ratio, *Int. J. Heat Mass Transfer* **27**, 1701–1713 (1984).
3. A. Storck and F. Coeuret, Mass transfer between a flowing fluid and a wall or immersed surface in fixed and fluidized beds, *Chem. Engng JI* **20**, 149–156 (1980).
4. M. V. Ramana Rao and C. Venkata Rao, Mass transfer in square channels: Part II—Ionic mass transfer in packed beds, *Indian J. Technol.* **8**, 44–47 (1970).
5. M. M. Melanson, Solid-phase radial heat transfer in stagnant packed beds for low tube to particle diameter ratios, M.S. thesis, Worcester Polytechnic Institute (1984).